



Published in final edited form as:

J Nucl Cardiol. 2010 ; 17(1): 27–37. doi:10.1007/s12350-009-9156-z.

Direct comparison of rest and adenosine stress myocardial perfusion CT with rest and stress SPECT

David R. Okada, BA^a, Brian B. Ghoshhajra, MD^a, Ron Blankstein, MD^{a,b}, Jose A. Rocha-Filho, MD^a, Leonid D. Shturman, MD^a, Ian S. Rogers, MD^a, Hiram G. Bezerra, MD^c, Ammar Sarwar, MD^{a,e}, Henry Gewirtz, MD^a, Udo Hoffmann, MD, PhD^a, Wilfred S. Mamuya, MD, PhD^{a,d}, Thomas J. Brady, MD^a, and Ricardo C. Cury, MD^{a,f}

^aCardiac MR PET CT Program, Department of Radiology and Division of Cardiology, Massachusetts General Hospital and Harvard Medical School, Boston, MA

^bNon-invasive Cardiovascular Imaging Program, Department of Medicine and Radiology, Brigham and Women's Hospital, Boston, MA

^cHarrington McLaughlin Heart and Vascular Institute, Case Western Reserve University, Cleveland, OH

^dLown Cardiovascular Group, Brookline, MA

^eDepartment of Radiology, Beth Israel Deaconess Medical Center and Harvard Medical School, Boston, MA

^fCardiovascular MR and CT Program, Baptist Cardiac and Vascular Institute, Miami, FL.

Abstract

Introduction—We have recently described a technique for assessing myocardial perfusion using adenosine-mediated stress imaging (CTP) with dual source computed tomography. SPECT myocardial perfusion imaging (SPECT-MPI) is a widely utilized and extensively validated method for assessing myocardial perfusion. The aim of this study was to determine the level of agreement between CTP and SPECT-MPI at rest and under stress on a per-segment, per-vessel, and per-patient basis.

Methods—Forty-seven consecutive patients underwent CTP and SPECT-MPI. Perfusion images were interpreted using the 17 segment AHA model and were scored on a 0 (normal) to 3 (abnormal) scale. Summed rest and stress scores were calculated for each vascular territory and patient by adding corresponding segmental scores.

Results—On a per-segment basis ($n = 799$), CTP and SPECT-MPI demonstrated excellent correlation: Goodman-Kruskall $\gamma = .59$ ($P < .0001$) for stress and $.75$ ($P < .0001$) for rest. On a per-vessel basis ($n = 141$), CTP and SPECT-MPI summed scores demonstrated good correlation: Pearson $r = .56$ ($P < .0001$) for stress and $.66$ ($P < .0001$) for rest. On a per-patient basis ($n = 47$), CTP and SPECT-MPI demonstrated good correlation: Pearson $r = .60$ ($P < .0001$) for stress and $.76$ ($P < .0001$) for rest.

Conclusions—CTP compares favorably with SPECT-MPI for detection, extent, and severity of myocardial perfusion defects at rest and stress.

Keywords

Adenosine; computed tomography (CT); ischemia; myocardial; sestamibi; SPECT

INTRODUCTION

Single photon emission computed tomography myocardial perfusion imaging (SPECT-MPI) is a widely utilized and extensively validated method for assessing myocardial perfusion. A significant body of data demonstrates the high diagnostic accuracy of MPI for the detection of myocardial ischemia and scar, and the determination of myocardial viability, as well as the prognostic value of MPI in predicting long-term cardiovascular outcomes.¹⁻¹¹

Rest myocardial computed tomography (CT) perfusion imaging has demonstrated good correlation with resting perfusion magnetic resonance imaging and histopathology for the detection of perfusion abnormalities in both human and animal studies.¹²⁻¹⁶ These results suggest that iodinated CT contrast medium has similar pharmacokinetics to gadolinium MRI contrast agents and demonstrates rapid early enhancement in healthy myocardium, relatively slow enhancement in ischemic territories, and markedly delayed washout in infarcted territories.¹⁷ These differential kinetics suggested the possibility of discriminating normal from abnormal myocardium, as well as differentiation of scar from ischemic myocardium.

Emerging animal and human data demonstrate good correlation of stress myocardial CT perfusion imaging with measurements of myocardial blood flow as defined by radionuclide microspheres and good diagnostic accuracy for the detection of obstructive coronary artery disease by comparison with invasive angiography.¹⁸⁻²¹ Our group has recently described a novel technique for assessing myocardial perfusion in humans using adenosine-mediated stress imaging (CTP) with dual source computed tomography (DSCT) that offers submillimeter spatial resolution and tomographic datasets.^{22,23}

However, comparison of a physiologic test with an anatomic gold standard is not ideal. The angiographic percent luminal narrowing of a stenosis does not always determine its hemodynamic significance. Furthermore, the physiologic effects of the number, shape, length, and location of coronary lesions can impact the hemodynamic significance of disease. Finally, patients with syndrome X or microvascular disease may have ischemia in the absence of angiographic abnormalities.

Thus, the aim of this study was to determine the level of agreement for presence and extent of perfusion abnormalities at stress and rest between CTP and MPI on a per-segment, per-vessel, and per-patient basis.

METHODS

Patient Population

Eligible participants for the study included 955 consecutive patients in our institution with age ≥ 40 years who underwent a nuclear stress test. Two populations were screened for eligibility: (1) all patients scheduled to undergo clinically indicated invasive angiography who have had a prior nuclear MPI within the previous 3 months; and (2) all patients who underwent nuclear MPI and were found to have high-risk features (i.e., high likelihood to be referred for invasive angiography). Exclusion criteria included renal insufficiency, unstable clinical status, asthma, critical aortic stenosis, and known allergy to iodinated contrast medium. Figure 1 demonstrates patient enrollment. The study was approved by our institutional review board and all subjects provided informed consent.

Image Acquisition

Comprehensive CT protocol—Patients were instructed to avoid caffeine products for a period of 24 h prior to the scan. Patients were not instructed to take or withhold any medications prior to the scan, and no beta blockers were given prior to or during the scan. Upon arrival to the CT suite, two IVs were placed (18 gauge for delivery of contrast and 20 gauge for infusion of adenosine) in the left and right antecubital veins. Adenosine was the only medication administered during the CT protocol.

CT acquisitions were performed on a dual-source 64-slice machine (Siemens Medical Systems: Definition, Forchheim, Germany) with a gantry rotation time of 330 ms. A flying focus along the z-axis (Z-sharp technology) and two 32-row detectors were used to acquire 64 overlapping .6 mm slices with a resulting temporal resolution of 83 ms.

The comprehensive CT protocol, including stress and rest acquisitions, is shown in Figure 2. First, scout images were obtained. Contrast timing was then determined using a test bolus of 10-15 mL of contrast. Flow rate for the test bolus and for image acquisition was 4-5 mL/s and was followed by a 20 cc flush of saline. Accordingly, for all scans, image acquisition timing was determined by adding 2-4 s to the time of peak opacification in the ascending aorta to account for the time necessary to perfuse the myocardium.

Adenosine infusion was then initiated at 140 mcg/kg/minutes. Three minutes later, a retrospectively ECG-gated scan with tube current modulation and pitch adaptation was obtained. Tube voltage (kV) and current (mA·s) were selected based on the body habitus of the patient. A tube voltage of 120 kV was used for most patients, while 100 kV was used for those with body mass index of ≤ 30 .

Average contrast dose ([iopamidol] Bracco Diagnostics: Isovue 370, Milan, Italy) for the stress acquisition was 65 cc delivered at a rate of 4-5 mL/s followed by a 20 cc saline flush. Patient symptoms, heart rate, blood pressure, and EKG were monitored by a cardiologist throughout the acquisition.

Immediately following the stress CT, adenosine infusion was discontinued. After an approximately 5 minutes interval to allow for resolution of symptoms and return of heart rate to baseline, resting CT images were acquired. To reduce contrast dose, a second timing bolus was not administered. Instead, the same delay that was used for stress acquisition was also used for rest acquisition. To reduce radiation exposure, rest CT utilized prospective triggering (Siemens: Sequential Scanning) at 65% of the RR interval. An infusion of 65-70 cc of iopamidol was administered at 4-5 mL/s followed by a 20 cc saline flush.

Contrast volumes for the rest and stress acquisitions were calculated according to both the patient's BMI and the scan length duration. Therefore, the average contrast dose for rest scans was higher than the average contrast dose for stress scans (66.3 cc vs. 67.3 cc) because acquisition in prospectively triggered mode occurred on every other heartbeat resulting in a longer scan length duration.

Nuclear stress testing—All nuclear SPECT imaging were performed according to standard institutional clinical protocols. Among the 47 study participants, 13 (28%) underwent adenosine SPECT while the remaining 34 (72%) had exercise SPECT. Among the 34 exercise stress tests, the average exercise time was 7 minutes and 10 seconds and the average workload achieved was 7.8 METS. The average percent of maximal predicted heart rate achieved (% MPHR) was 85.2%. Sixteen patients (4 of whom had $\leq 85\%$ MPHR) developed chest pain during the exam.

An adequate stress test was defined as either (1) achieving >85% of maximal predicted heart rate (MPHR), (2) any test utilizing adenosine, or (3) developing chest pain during exercise testing. Out of 47 stress tests, 38 (80%) were considered adequate. None of the patients who failed to achieve an adequate test had significant ECG changes during exercise.

Patients were injected with 10 mCi of Tc-99m sestamibi at rest and SPECT images were acquired with a dual-detector gamma camera, with 64 projections, each for 20 seconds, in a noncircular 180° orbit. In addition, an exercise or pharmacological stress test (IV adenosine infusion at 140 mcg/kg/minute for 5 minute) was performed, followed by an intravenous injection of 30 mCi of Tc-99m sestamibi. After 30-60 minutes, gated SPECT images were obtained.

Image Processing and Interpretation

SPECT-MPI—All SPECT-MPI images were analyzed by two experienced CBNC board certified independent readers (L.S., W.M.) and any areas of discrepancy were then resolved by a third experienced senior reader (H.G.). Using the 17 segment model recommended by ACC/AHA/ASNC,²⁴ semi-quantitative visual assessment of myocardial perfusion was performed using a 4-point scoring system (0 = normal; 1 = mild reduction of radioisotope uptake; 2 = moderate reduction of radioisotope uptake; 3 = severe reduction of radioisotope uptake). Rest and stress images were assessed. For each vascular territory summed rest and summed stress scores were calculated (SRS and SSS) by adding the corresponding scores, rest, and stress. For each patient, SRS and SSS were calculated by adding the corresponding scores for 17 segments, rest, and stress. Per-patient summed scores were then subdivided into three categories of perfusion abnormality: mild (0-3), moderate (4-12), and severe (≥ 13).

For each pair of stress and rest datasets, each of the 17 segments was scored for reversibility of perfusion abnormality as followed: 0 = no reversibility; 1 = minimal reversibility; 2 = partial reversibility; and 3 = complete reversibility.

CT perfusion—Prior to evaluation of perfusion, raw data were used to reconstruct stress and rest datasets at 65% of the RR interval using an extra smooth filter (Siemens B10) with slice thickness of .7 mm and overlap of .4 mm.

To ensure appropriate and consistent co-registration of all images, internal fiducial markers (e.g., mitral annular ring, left ventricular apex, pulmonary vasculature) and spatial localization coordinates available in the software (Circulation, Siemens Medical Systems, Germany) were used to co-register the stress and rest images.

For each dataset, a double oblique technique was used to create true short axis, 10 mm thick multiplanar reformats (MPR) images. Thicker slices were chosen as the increased voxel size results in decreased image noise and improve contrast resolution for visualization of normal and ischemic and infarcted myocardium.

For assessment of CT perfusion analysis, the standard ACC/AHA 17 segment model used for interpretation of SPECT was used. Semi-quantitative per segment analysis was performed by simultaneous visualization of short axis images obtained from stress and rest acquisitions. Narrow window and level setting were used (typically W200, L100) although the reading physician was allowed to adjust these display settings as needed.

After initial evaluation of thick MPR short axis images, readers were then allowed to examine multiphase cine data from the stress CT scan (available in 2 chamber, 4 chamber, and short axis views). Subsequently, global and regional wall motion abnormalities were noted. In addition any areas of questionable perfusion defects were examined in both systolic and

diastolic phases in order to differentiate potential artifacts (e.g., defect only present on one phase) from true perfusion defects (e.g., defect present on multiple phases and can be seen during both systole and diastole) and potentially associated to an area of regional wall motion abnormality.

All CT stress and rest images were independently analyzed by two experienced readers (R.B., R.C.C.) who were blinded to all patient and clinical data, including CT coronary angiographic findings. A joint consensus reading session was then performed to resolve any discrepancies and consensus was achieved in all cases.

For stress and rest images, each of the 17 segments was scored based on the absence or presence and severity of a perfusion defect. Perfusion defect severity was scored on a 0 (normal) to 3 (abnormal) scale. Summed rest and stress scores were calculated for each vascular territory and each patient by adding the corresponding segmental scores. To allow comparison of our data with recent data on the noninferiority of regadenoson stress SPECT to adenosine stress SPECT,²⁵ we further divided summed rest and stress scores into three categories of perfusion abnormality: mild (0-3), moderate (4-12), and severe (≥ 13).

For each pair of stress and rest datasets, each of the 17 segments was scored for reversibility of perfusion abnormality as followed: 0 = no reversibility; 1 = minimal reversibility; 2 = partial reversibility; and 3 = complete reversibility. Summed reversibility scores were calculated for each vascular territory and each patient by adding the corresponding segmental scores.

Radiation Dose

Effective radiation dose for each component of the DSCT examination (stress and rest) was calculated by multiplying the dose-length product (DLP) provided by scan console by a constant ($k = .017$ mSv/mGy/cm). In order to estimate radiation dose for SPECT-MPI, total megabecquerel was converted to millisievert (mSv).

Statistical Analysis

Data analysis was performed using SPSS version 17 (SPSS Inc., Chicago, IL). All continuous variables were expressed as mean \pm standard deviation while categorical variables were expressed as percentage. Correlations among continuous summed stress and rest scores were assessed using Pearson's correlation analysis. Correlations among nonsummed segmental scores were assessed using the Goodman-Kruskall gamma statistic. A P -value $<.05$ was considered statistically significant.

RESULTS

Patient Population

Table 1 summarizes baseline patient characteristics. Among the 47 study participants, the average age was 62.4 ± 10.2 years, 80.9% were male, 23.4% had diabetes 87.2% had hypertension, and 87.2% had dyslipidemia. The prevalence of obesity was 41.2% and the average BMI was 31.0 ± 5.6 kg/m². The prevalence of prior angina, myocardial infarction, and revascularization was 57.4%, 36.2% and 38.3%, respectively. Implantable cardioverter defibrillator (ICD) was the only cardiac device represented in the patient population. Two patients (4.3%) had an ICD.

Comprehensive CT Protocol

Adenosine stress CT was completed for all 47 patients within 26.9 ± 23.1 days after SPECT imaging. For one patient, the rest scan was not performed due to persisting angina following the adenosine DSCT stress exam.

Table 2 displays the scan parameters of each portion of the CT protocol. With the use of adenosine, the average heart rate increased from 66 ± 11 beats per minute at rest to 77 ± 13 beats per minute at stress while the average heart rate variability (defined as maximum heart rate minus minimum heart rate during acquisition) decreased from 18 to 16 beats per minute.

The average radiation exposure for the complete DSCT protocol was 12.3 ± 4.3 mSv and was nonsignificantly less than SPECT (12.4 ± 1.9 mSv; $P = .11$) (Figure 3).

CT stress perfusion defects were identified for 34 out of 47 patients (72%), 67 out of 141 vascular territories (48%), and 184 out of 799 myocardial segments (23%). Out of the 67 vascular territories with abnormal CT stress perfusion for which CT rest images were obtained, 14 (21%) were fixed, 19 (28%) were fully reversible, and 31 (46%) were partially reversible. The average SSS was 7.0, and the average SRS was 3.0.

SPECT-MPI Findings

On SPECT-MPI, 35 of the 47 patients (74%), 53 of the 141 vascular territories (38%), and 156 of the 799 myocardial segments (20%) had perfusion abnormalities during stress. Out of 53 vascular territories with abnormal SPECT-MPI, 11 (21%) were fixed, 24 (45%) were fully reversible, and 18 (34%) were partially reversible. The average SSS was 5.1 and the average SRS was 2.4.

Direct Comparison of CTP and MPI

On a per-segment basis ($n = 799$ for stress and $n = 782$ for rest), CTP and MPI demonstrated an excellent correlation: Goodman-Kruskall $\gamma = .59$ ($P < .0001$) for stress and $.75$ ($P < .0001$) for rest. On a per-vessel basis ($n = 141$ for stress and $n = 138$ for rest), CTP and MPI summed scores demonstrated a good correlation: Pearson $r = .56$ ($P < .0001$) for stress and $.66$ ($P < .0001$) for rest. On a per-patient basis ($n = 47$ for stress and $n = 46$ for rest), CTP and MPI demonstrated a good correlation: Pearson $r = .60$ ($P < .0001$) for stress and $.76$ ($P < .0001$) for rest. Figure 4 shows an example of good qualitative correlation between the two modalities.

Agreement between CTP and MPI to determine the severity of perfusion abnormalities using three categories based on summed scores was 76% for stress and 88% for rest on a per vessel basis and 57% for stress and 78% for rest on a per patient basis (Figure 5).

DISCUSSION

In this direct comparison of two modalities of stress and rest MPI in patients, we demonstrated an excellent correlation between CTP and SPECT for the detection of perfusion abnormalities and for the assessment of defect severity on a per-segment, per-vessel, and per-patient basis.

Myocardial perfusion imaging with ^{201}Tl and $^{99\text{m}}\text{Tc}$ MIBI during exercise or pharmacologic stress enables the noninvasive detection of perfusion defects and can provide indirect assessment of coronary anatomy with a high degree of sensitivity and specificity.⁴⁻⁷ Furthermore, nuclear testing provides valuable prognostic information about patients with known or suspected CAD and predicts functional recovery following coronary revascularization.⁸⁻¹⁰ Finally, nuclear imaging has proven useful in determining which patients are most likely to benefit from coronary revascularization.¹¹

At the same time, SPECT is limited by a spatial resolution of approximately 10 mm, artifacts arising from gastric activity, breast attenuation, and diaphragmatic attenuation, and susceptibility to “false negative” studies in cases of balanced ischemia (triple-vessel disease).²⁶ Furthermore, SPECT is limited to the visualization of perfusion without direct information about coronary anatomy.

Contrast-enhanced gradient echo cardiac MRI represents an alternative modality for assessing rest and pharmacologically induced stress myocardial perfusion and has demonstrated excellent diagnostic accuracy for the detection of hemodynamically significant coronary artery disease.^{27,28} However, stress cardiac MRI studies take significantly longer than the CTP protocol utilized in this study, and stress cardiac MRI is not widely clinically available. Further, patients with implantable cardioverter-defibrillators or other ferromagnetic implanted devices, or who have a history of claustrophobia, may be contraindicated for cardiac MRI.

A number of recent studies have demonstrated the similarities between the myocardial pharmacokinetic similarities between gadolinium MRI contrast agents and iodinated CT contrast agents.¹²⁻¹⁷ Compared with normal myocardium, ischemic myocardium demonstrates relatively slow iodinated contrast enhancement while fibrotic tissue in territories of prior infarcts demonstrates delayed enhancement with markedly delayed wash-in and wash-out.

We have recently described a novel protocol for evaluating adenosine-mediated stress myocardial perfusion using DSCT.^{22,23} In an initial experience, we demonstrated CTP to be feasible with good image quality. Furthermore, CTP demonstrated a good diagnostic accuracy for the detection of obstructive coronary artery disease using $\geq 50\%$ luminal narrowing at quantitative invasive angiography as the reference standard. Specifically, CTP demonstrated a sensitivity of 79% and a specificity of 80% versus invasive angiography. The total dose of iodinated contrast for CTP varied with scan length duration and patient BMI, and ranged from 140 to 165 cc, which is significantly higher than the dose associated with clinical coronary CT angiography or invasive coronary angiography.

Historically, invasive angiography is commonly utilized as the reference standard for evaluating the diagnostic accuracy of perfusion imaging modalities for the detection of flow-limiting CAD.^{1-3,6,29} However, comparison of a physiologic test to an anatomic reference standard is not ideal. Patients with microvascular disease (syndrome X) may have perfusion deficits but angiographically normal coronary arteries.³⁰ Furthermore, the angiographically determined percent luminal narrowing does not always correspond to the physiologic significance of the disease. Furthermore, the physiologic effects of the number in series, shape, length, and location of coronary lesions can impact the hemodynamic significance of disease.

The current study directly compares CTP and SPECT on a per-segment, per-vessel, and per-patient basis. A total of 799 segments were compared. Since both tests are physiologic in nature and both modalities provide tomographic datasets, we were able to perform a segment-to-segment comparison that would not have been possible using invasive angiography as a reference standard. This head-to-head approach has been previously used in the validation of ^{99m}Tc-Sestamibi, ^{99m}Tc-Tetrofosmin as myocardial perfusion agents.^{4,31,32}

The level of concordance between the two modalities is both technically and clinically interesting since CTP offers a superior sub-millimeter spatial resolution and the ability to simultaneously visualize coronary artery anatomy and myocardial perfusion in a single examination.

In addition, CTP utilizes the two independent x-ray sources of a dual-source scanner with a resulting temporal resolution for stress acquisitions of 83 ms. Beta blockers were not administered prior to or during the scan and adenosine caused an increase in average heart rate from 66 ± 12 to 77 ± 13 beats per minute. However, the superior temporal resolution provided adequate image quality at heart rates as high as 80-90 beats per minute. Still, it should be acknowledged that patients with high resting heart rates and marked increases in heart rate during adenosine administration pose a potential challenge for CTP image quality.

The segment-to-segment analysis provided the most direct comparison of CTP and SPECT. We observed an excellent correlation with a Goodman and Kruskal gamma value of .59 ($P < .0001$) for stress and .75 ($P < .0001$) for rest.

Differences in spatial resolution and occasional difference in cardiac phase between the two modalities likely resulted in segmental misregistration in isolated cases, thus decreasing the goodness of correlation. Furthermore, it should be noted that CTP is subject to a number of unique artifacts, including beam hardening, which results from attenuation of x-rays by highly dense structures like the vertebral body or descending aorta, affecting particularly the basal infero-lateral wall. Finally, it remains unclear what the optimal parameters are for CTP analysis, including window width and level, cardiac phase, slice thickness, and reconstruction algorithm.

We summed the segmental scores in order to perform per-vessel and per-patient analyses. On a per-vessel basis, CTP and MPI summed scores demonstrated a good correlation: Pearson $r = .56$ ($P < .0001$) for stress and $.66$ ($P < .0001$) for rest. On a per-patient basis, CTP and MPI demonstrated a good correlation: Pearson $r = .60$ ($P = .008$) for stress and $.76$ ($P < .0001$) for rest.

Recent studies comparing SPECT with adenosine-mediated stress versus A_{2A} -specific regadenoson-mediated stress serve to put our correlation values into an appropriate perspective.^{25,33} Iskandrian and co-workers assessed the strength of agreement between both sequential adenosine images and sequential adenosine-regadenoson images. Using the standard 17 segment model,²⁴ these authors graded each myocardial segment for the presence or absence of a reversible perfusion defect across sequential studies. They then classified each patient according to three ischemic categories based on the number of segmental reversible defects: 0-1, 2-4, or ≥ 5 defects. Averaging across these categories without weighting for the number of data points in each, sequential adenosine-adenosine scans showed a rate of agreement of 64% and sequential adenosine-regadenoson scans showed a rate of agreement of 63%. Thus, even using the same imaging modality, imaging agent, and vasodilator, there still is some lack of reproducibility.

In a similar fashion, we further analyzed our summed stress and rest scores in terms of three ischemic categories on a per-vessel and per-patient basis: mild (0-3), moderate (4-12), and severe (≥ 13). Averaging across the three categories and weighting for the number of data points in each, we observed a rate of agreement of 76% between CTP and SPECT stress images, and a rate of agreement of 88% between CTP and SPECT rest images on a per-vessel basis. On a per-patient basis, we observed a rate of agreement of 57% between CTP and SPECT stress images, and a rate of agreement of 78% between CTP and SPECT rest images.

Study Limitations

This study was a single-center, single-vendor trial and the results should be further validated by multicenter and multivendor trials. Second, not all of the patients enrolled in our study achieved adequate stress during their SPECT examinations, which could lead to an underestimation of the presence and extent of perfusion defects. Third, while we were able to mitigate verification bias by including patients irrespective of whether they underwent invasive angiography, we did not study any truly normal patients as a control group. On the other hand, the study group did represent the typical population referred for noninvasive testing. Fourth, although good image quality was achieved in the two patients in this study with an ICD, beam hardening due to cardiac device leads should be noted as a potential source of poor CTP image quality. Fifth, although the 83 ms temporal resolution of the dual-source scanner utilized by the CTP protocol enabled good image quality at heart rates as high as 80-90 beats per minute, patients with high resting heart rates and marked increases in heart rate during adenosine infusion pose an additional potential challenge for CTP image quality, particularly if these

patients are not on chronic beta blockade. Sixth, the total dose of contrast medium for CTP was 140-165 cc, which is significantly greater than the dye load associated with clinical coronary CT angiography or invasive coronary angiography. Finally, our patient population was predominantly Caucasian and predominantly male. It will be important to validate our results across genders and ethnicities.

CONCLUSIONS

SPECT is the mostly widely utilized technique for assessing myocardial perfusion. The current study validates the ability of CTP to assess myocardial perfusion at rest and during adenosine, when compared directly to SPECT. Thus, with a single study and with no increase in radiation, one can assess myocardial perfusion and coronary anatomy simultaneously.

We conclude that adenosine-mediated stress MPI with DSCT compares well with nuclear stress testing in a direct correlation of segments, vascular territories, and patients, and is feasible with a radiation dose that is not significantly different from SPECT. Larger multicenter trials will need to be performed to confirm the results of this initial study.

Acknowledgments

The authors would like to thank the CT technologists, the Radiology department nursing staff, and the staff physicians in the Division of Cardiology at the Massachusetts General Hospital.

Funding sources: This study is supported in part by a grant from Astellas Pharma, Inc. Drs Blankstein, Ghoshhajra, Shturman, and Rogers have received support from NIH grant 1T32 HL076136. Dr Ghoshhajra has received support from RSNA 213740. Dr Cury reports receiving research grant support from Astellas, Pharma, Inc.

References

1. Bailey IK, Griffith LS, Rouleau J, Strauss W, Pitt B. Thallium-201 myocardial perfusion imaging at rest and during exercise. Comparative sensitivity to electrocardiography in coronary artery disease. *Circulation* 1977;55:79–87. [PubMed: 830222]
2. Verani MS, Marcus ML, Razzak MA, Ehrhardt JC. Sensitivity and specificity of thallium-201 perfusion scintigrams under exercise in the diagnosis of coronary artery disease. *J Nucl Med* 1978;19:773–82. [PubMed: 660279]
3. Okada RD, Boucher CA, Pohost GM. Quantitative split dose thallium-201 imaging with exercise: A technique for obtaining rest and exercise perfusion images in one setting and markedly reducing the study time. *J Am Coll Cardiol* 1985;5:70–7. [PubMed: 3880568]
4. Wackers FJ, Berman DS, Maddahi J, Watson DD, Beller GA, Strauss HW, et al. Technetium-99m hexakis 2-methoxyisobutyl isonitrile: Human biodistribution, dosimetry, safety, and preliminary comparison to thallium-201 for myocardial perfusion imaging. *J Nucl Med* 1989;30:301–11. [PubMed: 2525610]
5. Kahn JK, McGhie I, Akers MS, Sills MN, Faber TL, Kulkarni PV, et al. Quantitative rotational tomography with 201Tl and 99mTc 2-methoxy-isobutyl-isonitrile. A direct comparison in normal individuals and patients with coronary artery disease. *Circulation* 1989;79:1282–93. [PubMed: 2785873]
6. Nguyen T, Heo J, Ogilby JD, Iskandrian AS. Single photon emission computed tomography with thallium-201 during adenosine-induced coronary hyperemia: Correlation with coronary arteriography, exercise thallium imaging and two-dimensional echocardiography. *J Am Coll Cardiol* 1990;16:1375–83. [PubMed: 2229789]
7. Rocco TP, Dilsizian V, Strauss HW, Boucher CA. Technetium-99m isonitrile myocardial uptake at rest. II. Relation to clinical markers of potential viability. *J Am Coll Cardiol* 1989;14:1678–84. [PubMed: 2584556]

8. Leppo JA, O'Brien J, Rothendler JA, Getchell JD, Lee VW. Dipyridamole-thallium-201 scintigraphy in the prediction of future cardiac events after acute myocardial infarction. *N Engl J Med* 1984;310:1014–8. [PubMed: 6708976]
9. Berman DS, Hachamovitch R, Kiat H, Cohen I, Cabico JA, Wang FP, et al. Incremental value of prognostic testing in patients with known or suspected ischemic heart disease: A basis for optimal utilization of exercise technetium-99m sestamibi myocardial perfusion single-photon emission computed tomography. *J Am Coll Cardiol* 1995;26:639–47. [PubMed: 7642853]
10. Hachamovitch R, Berman DS, Kiat H, Cohen I, Cabico JA, Friedman J, et al. Exercise myocardial perfusion SPECT in patients without known coronary artery disease: Incremental prognostic value and use in risk stratification. *Circulation* 1996;93:905–14. [PubMed: 8598081]
11. Hachamovitch R, Berman DS, Shaw LJ, Kiat H, Cohen I, Cabico JA, et al. Incremental prognostic value of myocardial perfusion single photon emission computed tomography for the prediction of cardiac death: Differential stratification for risk of cardiac death and myocardial infarction. *Circulation* 1998;97:535–43. [PubMed: 9494023]
12. Cury RC, Nieman K, Shapiro MD, Butler J, Nomura CH, Ferencik M, et al. Comprehensive assessment of myocardial perfusion defects, regional wall motion, and left ventricular function by using 64-section multidetector CT. *Radiology* 2008;248:466–75. [PubMed: 18641250]
13. Hoffmann U, Millea R, Enzweiler C, Ferencik M, Gulick S, Titus J, et al. Acute myocardial infarction: Contrast-enhanced multidetector row CT in a porcine model. *Radiology* 2004;231:697–701. [PubMed: 15118118]
14. Mahnken AH, Bruners P, Katoh M, Wildberger JE, Gunther RW, Buecker A. Dynamic multi-section CT imaging in acute myocardial infarction: Preliminary animal experience. *Eur Radiol* 2006;16:746–52. [PubMed: 16283323]
15. Nieman K, Shapiro MD, Ferencik M, Nomura CH, Abbara S, Hoffmann U, et al. Reperfused myocardial infarction: Contrast-enhanced 64-Section CT in comparison to MR imaging. *Radiology* 2008;247:49–56. [PubMed: 18372464]
16. Ruzsics B, Lee H, Zwerner PL, Gebregziabher M, Costello P, Schoepf UJ. Dual-energy CT of the heart for diagnosing coronary artery stenosis and myocardial ischemia-initial experience. *Eur Radiol* 2008;18:2414–24. [PubMed: 18523782]
17. Gerber BL, Belge B, Legros GJ, Lim P, Poncelet A, Pasquet A, et al. Characterization of acute and chronic myocardial infarcts by multidetector computed tomography: Comparison with contrast-enhanced magnetic resonance. *Circulation* 2006;113:823–33. [PubMed: 16461822]
18. George RT, Jerosch-Herold M, Silva C, Kitagawa K, Bluemke DA, Lima JA, et al. Quantification of myocardial perfusion using dynamic 64-detector computed tomography. *Invest Radiol* 2007;42:815–22. [PubMed: 18007153]
19. George RT, Silva C, Cordeiro MA, DiPaula A, Thompson DR, McCarthy WF, et al. Multidetector computed tomography myocardial perfusion imaging during adenosine stress. *J Am Coll Cardiol* 2006;48:153–60. [PubMed: 16814661]
20. Kurata A, Mochizuki T, Koyama Y, Haraikawa T, Suzuki J, Shigematsu Y, et al. Myocardial perfusion imaging using adenosine triphosphate stress multi-slice spiral computed tomography: Alternative to stress myocardial perfusion scintigraphy. *Circ J* 2005;69:550–7. [PubMed: 15849441]
21. George RT, Arbab-Zadeh A, Miller JM, Kitagawa K, Chang H-J, Bluemke DA, Becker L, et al. Adenosine stress 64- and 256-row detector computed tomography angiography and perfusion imaging: A pilot study evaluating the transmural extent of perfusion abnormalities to predict atherosclerosis causing myocardial ischemia. *Circ Cardiovasc Imaging* 2009;2:174–82. [PubMed: 19808590]
22. Blankstein R, Shturman LD, Rogers IS, Rocha-Filho JA, Okada DR, Sarwar A, et al. Adenosine induced stress myocardial perfusion imaging using dual source cardiac computed tomography. *J Am Coll Cardiol* 2009;54:1072–84. [PubMed: 19744616]
23. Blankstein R, Okada DR, Rocha-Filho JA, Rybicki F, Brady TJ, Cury RC. Cardiac myocardial perfusion imaging using dual source computed tomography. *Int J Cardiovasc Imaging* 2009;25:209–16. [PubMed: 19051056]
24. Cerqueira MD, Weissman NJ, Dilsizian V, Jacobs AK, Kaul S, Laskey WK, et al. Standardized myocardial segmentation and nomenclature for tomographic imaging of the heart: A statement for

- healthcare professionals from the Cardiac Imaging Committee of the Council on Clinical Cardiology of the American Heart Association. *Circulation* 2002;105:539–42. [PubMed: 11815441]
25. Iskandrian AE, Bateman TM, Belardinelli L, Blackburn B, Cerqueira MD, Hendel RC, et al. Adenosine versus regadenoson comparative evaluation in myocardial perfusion imaging: Results of the ADVANCE phase 3 multicenter international trial. *J Nucl Cardiol* 2007;14:645–58. [PubMed: 17826318]
 26. DePuey EG, Garcia EV. Optimal specificity of thallium-201 SPECT through recognition of imaging artifacts. *J Nucl Med* 1989;30:441–9. [PubMed: 2661749]
 27. Klem I, Greulich S, Heitner JF, Kim H, Vogelsberg H, Kispert EM, et al. Value of cardiovascular magnetic resonance stress perfusion testing for the detection of coronary artery disease in women. *JACC Cardiovasc Imaging* 2008;1:436–45. [PubMed: 19356464]
 28. Rieber J, Huber A, Erhard I, Mueller S, Schweyer M, Koenig A, et al. Cardiac magnetic resonance perfusion imaging for the functional assessment of coronary artery disease: A comparison with coronary angiography and fractional flow reserve. *Eur Heart J* 2006;27:1465–71. [PubMed: 16720685]
 29. Prigent F, Maddahi J, Garcia E, Van Train K, Friedman J, Berman D. Noninvasive quantification of the extent of jeopardized myocardium in patients with single-vessel coronary disease by stress thallium-201 single-photon emission computerized rotational tomography. *Am Heart J* 1986;111:578–86. [PubMed: 3485369]
 30. Fragasso G, Rossetti E, Dosio F, Gianolli L, Pizzetti G, Cattaneo N, et al. High prevalence of the thallium-201 reverse redistribution phenomenon in patients with syndrome X. *Eur Heart J* 1996;17:1482–7. [PubMed: 8909903]
 31. Kiat H, Maddahi J, Roy LT, Van Train K, Friedman J, Resser K, et al. Comparison of technetium 99m methoxy isobutyl isonitrile and thallium 201 for evaluation of coronary artery disease by planar and tomographic methods. *Am Heart J* 1989;117:1–11. [PubMed: 2643279]
 32. Matsunari I, Fujino S, Taki J, Senma J, Aoyama T, Wakasugi T, et al. Comparison of defect size between thallium-201 and technetium-99m tetrofosmin myocardial single-photon emission computed tomography in patients with single-vessel coronary artery disease. *Am J Cardiol* 1996;77:350–4. [PubMed: 8602561]
 33. Hendel RC, Bateman TM, Cerqueira MD, Iskandrian AE, Leppo JA, Blackburn B, et al. Initial clinical experience with regadenoson, a novel selective A2A agonist for pharmacologic stress single-photon emission computed tomography myocardial perfusion imaging. *J Am Coll Cardiol* 2005;46:2069–75. [PubMed: 16325044]

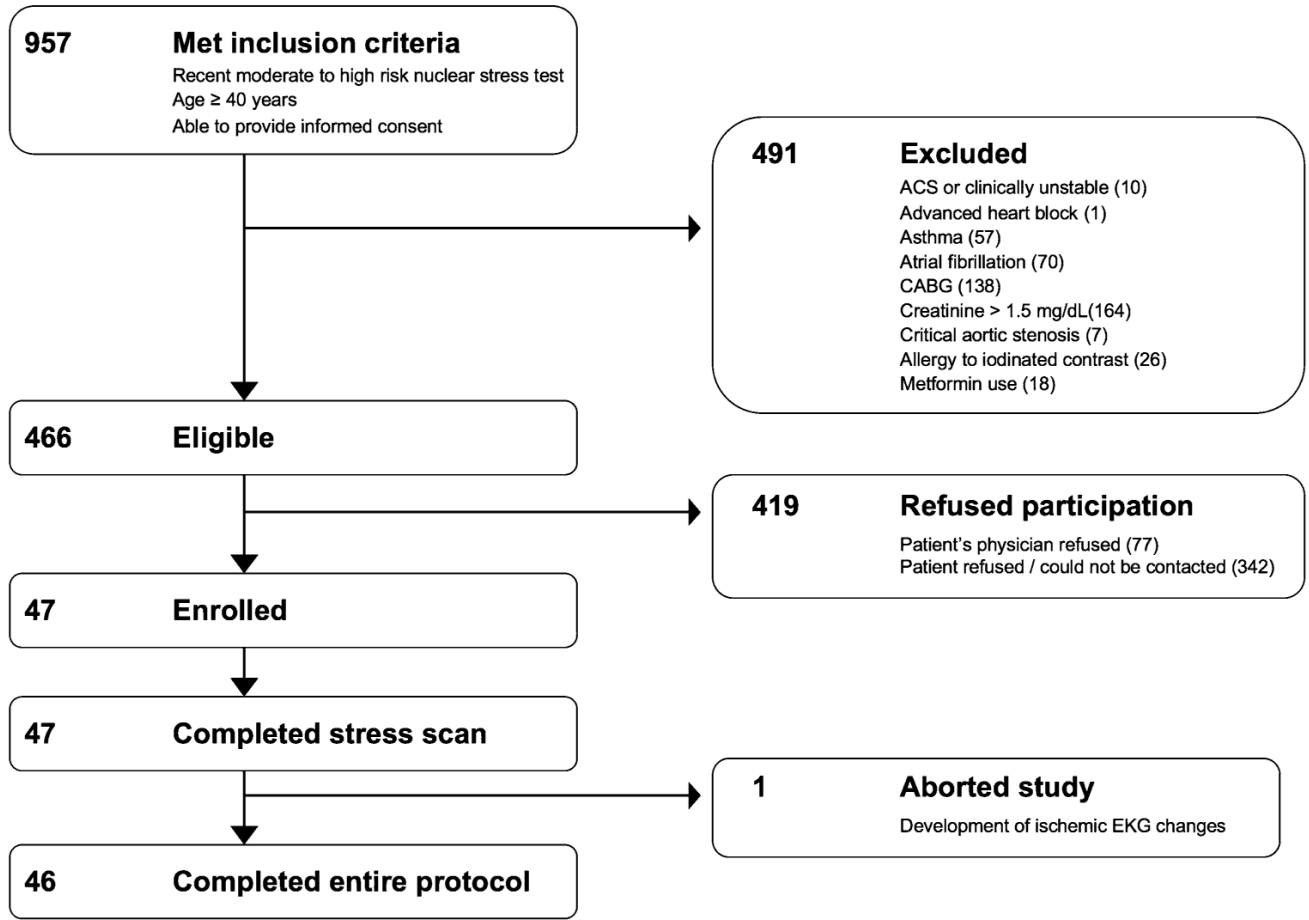


Figure 1. Patient recruitment. Out of 957 patients meeting inclusion criteria, 491 were excluded and 419 refused to participate. Forty-seven patients completed the CT stress perfusion scan. ACS Acute coronary syndrome, CABG coronary artery bypass grafting surgery.

Stress Perfusion CT Protocol

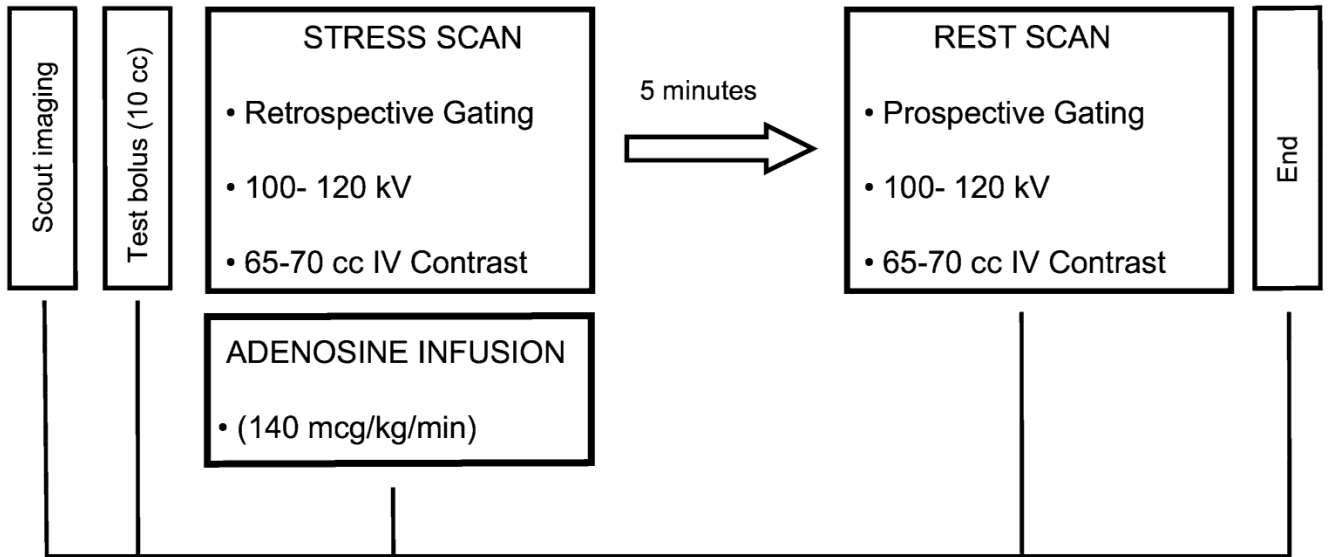


Figure 2. Stress Myocardial CT Perfusion Protocol. See “Methods” section for further detail.

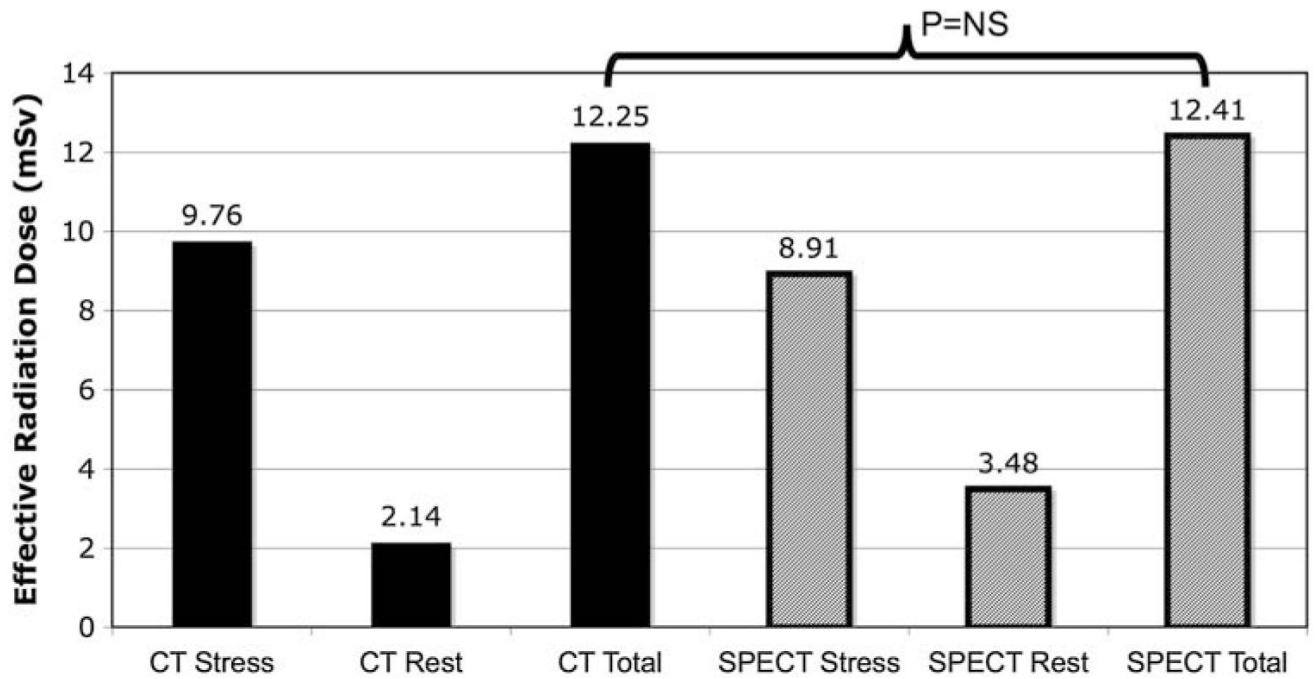


Figure 3. Radiation exposure of CT perfusion versus SPECT-MPI. Estimated effective radiation dose in millisivert (mSv) is displayed for CTP (*solid bars*) and SPECT (*striped bars*). The total effective radiation dose was not statistically different between the two modalities.

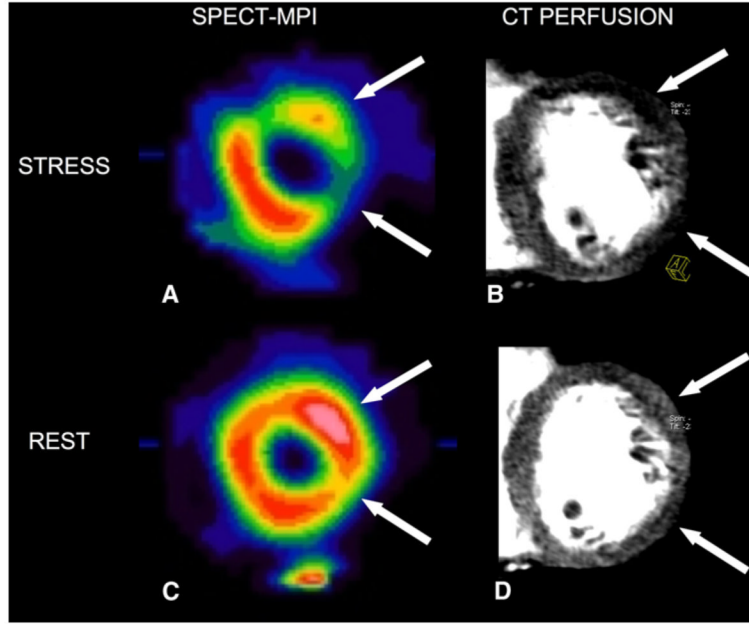


Figure 4. Example of correlation between CTP and SPECT. A 53-year-old male with a history of non-ST segment elevation myocardial infarction presenting with exertional chest pain. Short axis views at the mid-ventricular level of adenosine-mediated sestamibi SPECT showing large fully reversible perfusion defects of the lateral wall suggestive of moderate ischemia (panels **A** and **C**; *white arrows*). Short axis thick multiplanar reformatted (MPR) 8-mm thick slices at the mid-ventricular level of adenosine-mediated CTP showing extensive reversible perfusion defects of the lateral wall (panels **B** and **D**; *white arrows*).

A. Stress Perfusion Defect Severity (SSS) in 141 Vascular Territories		CT Perfusion		
		Mild	Moderate	Severe
SPECT	Mild	94	22	1
	Moderate	10	12	1
	Severe	0	0	1

B. Rest Perfusion Defect Severity (SRS) in 138 Vascular Territories		CT Perfusion		
		Mild	Moderate	Severe
SPECT	Mild	118	10	0
	Moderate	6	3	0
	Severe	0	0	1

C. Stress Perfusion Defect Severity (SSS) in 47 Patients		CT Perfusion		
		Mild	Moderate	Severe
SPECT	Mild	13	9	1
	Moderate	6	11	4
	Severe	0	0	3

D. Rest Perfusion Defect Severity (SRS) in 46 Patients		CT Perfusion		
		Mild	Moderate	Severe
SPECT	Mild	29	8	0
	Moderate	2	5	0
	Severe	0	0	2

Figure 5.

Agreement of CTP and SPECT for the Assessment of Perfusion Defect Severity on a per-vessel and per-patient Basis Using 3 Ischemic Categories. Summed stress and scores (SSS) were used to categorize each of 141 vascular territories as mild (SSS of 0-3), moderate (SSS of 4-12), or severe (SSS of ≥ 13) (panel **A**). Summed rest scores (SRS) were similarly used to categorize territories as mild, moderate and severe (panel **B**). Summed rest and stress scores were then used to categories each of 47 patients as mild, moderate, or severe (panels **C** and **D**).

Table 1

Baseline characteristics

Characteristics	Total (n = 47)
Demographics	
Age (years)	62.4 ± 10.2
Male gender (%)	80.9
BMI (kg/m ²)	31.0 ± 5.6
Obesity (BMI ≥ 30) (%)	41.2
Ethnicity (%)	
Caucasian	82.9
Black	4.3
Hispanic	12.8
Tobacco (%)	
Current	14.9
Former	53.2
Never	31.9
Medical history (%)	
Diabetes mellitus*	23.4
Hypertension	87.2
Dyslipidemia*	87.2
Family history of CAD*	40.4
Previous angina	57.4
Prior myocardial infarction	36.2
Prior coronary revascularization	38.3
Biomarkers (mg/dL)	
Total cholesterol	167.0 ± 60.5
HDL-cholesterol	46.5 ± 17.5
LDL-cholesterol	102.6 ± 44.3
Serum triglycerides	150.9 ± 70.0
Serum creatinine	1.1 ± 0.2
Medications (%)	
Aspirin	63.8
Beta blocker	74.5
Statin	76.7
Vital signs	
Systolic blood pressure (mmHg)	137.1 ± 18.8
Diastolic blood pressure (mmHg)	76.7 ± 10.3
Heart rate (bpm)	65.9 ± 11.9

* Family history, diabetes, and dyslipidemia classified per documentation in cardiologist note *BMI* Body mass index

Table 2

CT perfusion scan parameters

Parameter	Stress	Rest
Heart rate (beat per minute)		
Min	70 ± 15	57 ± 12
Max	86 ± 21	76 ± 17
Mean	77 ± 13	66 ± 12
Mean variability (max – min)	16 ± 22	18 ± 18
Scan acquisition time (seconds)	7 ± 3	11 ± 4
Pitch	.35 ± .08	-
kV	100-120	100-120
mAs (stress)/mA* (rest)	330-370	150-258
Effective radiation exposure (mSv)	10.0 ± 4.0	2.2 ± .7
Contrast dose (cc)	66 ± 3	67 ± 3

* For retrospective triggering (helical scanning), mAs = total tube current × gantry rotation time [~.33 s]; for prospective triggering (sequential scanning), mA = total tube current × exposure time [~.2 s]